

# EFFECTS OF EARLY COSMIC REIONIZATION ON THE SUBSTRUCTURE PROBLEM IN GALACTIC HALO

HAJIME SUSA<sup>1</sup>

DEPARTMENT OF PHYSICS, RIKKYO UNIVERSITY, NISHI-IKEBUKURO, TOSHIMAKU, JAPAN

MASAYUKI UMEMURA<sup>2</sup>

CENTER FOR COMPUTATIONAL SCIENCES, UNIVERSITY OF TSUKUBA, JAPAN

<sup>1</sup> SUSA@RIKKYO.AC.JP

<sup>2</sup> UMEMURA@RCCP.TSUKUBA.AC.JP

*Draft version June 30, 2018*

## ABSTRACT

Recent observations on the cosmic microwave background by *Wilkinson Microwave Anisotropy Probe* (*WMAP*) strongly suggest that the reionization of the universe took place quite early ( $z \sim 17$ ). On the other hand, it has been pointed out that the cold dark matter cosmology suffers from the substructure problem that subgalactic halos are overproduced than the observed dwarf galaxies in the Local Group. In this paper, as a potential mechanism to solve this problem, we consider the feedback effects of the early reionization on the formation of small-scale structures. For this purpose, we perform 3D radiation hydrodynamic simulations with incorporating the radiative transfer for ionizing photons. As a result, it is found that the early reionization is so devastating for low-mass systems with  $M_{\text{vir}} \lesssim 10^8 M_{\odot}$  or  $v_{\text{circ}} \lesssim 20 \text{ km s}^{-1}$ , and almost all gas is photo-evaporated in more than 95% of low-mass systems. Such a strong negative feedback on the formation of low-mass galaxies may solve the substructure problem and support the picture that Local Group dwarf galaxies are descendants of the more massive halos that experienced and survived tidal stripping.

*Subject headings:* galaxies: formation — galaxies: dwarf — radiative transfer — molecular processes — hydrodynamics

## 1. INTRODUCTION

It has been claimed that too many subgalactic halos are formed in a cold dark matter (CDM) universe, compared to the dwarf galaxies observed in the Local Group (Klypin et al. 1999; Moore et al. 1999). One of the simplest ways to resolve this discrepancy is the exclusion of baryonic matter from small halos by some feedback mechanisms. The mechanisms could be either the gas ejection due to energy input by the multiple supernova (SN) explosions (Dekel & Silk 1986; Yepes et al. 1997; Efstathiou 2000; Kay et al. 2002; Marri & White 2002; Wada & Venkatesan 2003; Ricotti & Ostriker 2004) or the photo-evaporation by ultraviolet background (UVB) radiation (Umemura & Ikeuchi 1984; Bond, Szalay & Silk 1988; Efstathiou 1992; Babul & Rees 1992; Thoul & Weinberg 1996; Barkana & Loeb 1999; Kitayama & Ikeuchi 2000; Kitayama et al. 2000, 2001; Bullock et al. 2000; Somerville 2002; Benson et al. 2002; Ricotti, Gnedin, & Shull 2002; Susa & Umemura 2004). As for the former process, Wada & Venkatesan (2003) recently performed high resolution hydrodynamic simulations and concluded that 1000 SNe are required in order to disrupt a galaxy with  $M \sim 10^8 M_{\odot}$  at  $z \sim 10$ , while only 100 SNe in the halo lead to triggering the recollapse of the whole system. These results show that SN explosions are not always destructive for the formation of low-mass galaxies, although it depends upon the initial mass function of stars (e.g. Ricotti & Ostriker 2004). On the other hand, the previous studies on the UVB feedback have shown that the photo-evaporation by UVB is depen-

dent upon the virial mass. As long as systems are more massive than  $\approx 10^8 M_{\odot}$ , the photo-evaporation by UVB is not effective, because deep potential wells can retain the ionized gas. However, at smaller mass-scales, the feedback by UVB is expected to play a very important role. Recently, *Wilkinson Microwave Anisotropy Probe* (*WMAP*) (Kogut et al. 2003) suggested that the universe was reionized in a rather early epoch ( $z \sim 17$ ). If this is the case, the UVB feedback could be quite effective for low-mass systems, since density fluctuations are photo-heated before they collapse to form stars.

Very recently, Kravtsov, Gnedin & Klypin (2004) analyzed the dynamical history of small substructure halos with present mass  $\lesssim 10^{8-9} M_{\odot}$  by a cosmological simulation. They found that 10% of small halos originate in considerably larger systems with  $\gtrsim 10^9 M_{\odot}$ , which survived the tidal stripping. They suggest that the Galactic satellites are descendants of relatively massive systems which formed at higher redshifts and did not significantly suffer from the UVB. This argument is plausible, if systems with  $\gtrsim 10^9 M_{\odot}$  are impervious even to the early reionization, and also the star formation in low-mass systems is completely suppressed.

Kitayama et al. (2001) have investigated the UVB feedback by one dimensional radiation hydrodynamic simulation for halos which collapse at  $z \lesssim 10$ , and found that the central parts cannot cool down to form stars if the virial temperature is less than  $10^4 \text{ K}$  and  $I_{21} \gtrsim 10^{-2}$ , where  $I_{21}$  is the intensity at Lyman limit in units of  $10^{-21} \text{ erg s}^{-1} \text{ cm}^{-1} \text{ Hz}^{-1} \text{ str}^{-1}$ . Dijkstra et al. (2004) extended this

work to higher redshifts by one dimensional hydrodynamic calculations, and found that gas is not photo-evaporated in halos with circular velocities of  $10\text{--}20\text{ km s}^{-1}$  at  $z > 10$ . But, in the hierarchical structure formation in a cold dark matter universe, three-dimensional (3D) time-dependent self-shielding is significant for the UVB feedback, as shown by Susa & Umemura (2004). In particular, such radiative transfer effects are likely to be essential, when the reionization proceeds at higher redshifts (in higher density intergalactic matter).

In this paper, we perform 3D radiation hydrodynamic simulations with solving the radiative transfer for ionizing photons, and attempt to elucidate the feedback effects of the early reionization on the formation of subgalactic systems. In the next section, the method of numerical simulations is briefly described, and the assumption for ionizing radiation intensity is provided. In §3, we present the numerical results for UVB feedback and also make the convergence check of the results. §4 is devoted to the discussion on the substructure problem.

## 2. NUMERICAL METHOD

The details of numerical method is given in Susa & Umemura (2004). Here, we briefly describe the model and method for simulations.

Hydrodynamics is calculated by Smoothed Particle Hydrodynamics (SPH) method. We use the version of SPH by Umemura (1993) with the modification according to Steinmetz & Müller (1993), and also we adopt the particle resizing formalism by Thacker et al. (2000). The gravitational force is calculated by a special purpose processor for gravity, GRAPE-6 (Makino 2002). In order to access GRAPE boards, we utilize the Heterogeneous Multi-Computer System (HMCS) (Boku et al. 2002) which allows us to use GRAPE in parallel processors such as PC clusters.

The softening length for gravity is set to be 20pc for SPH and CDM particles. This value is based on the convergence test shown in section 3. The non-equilibrium chemistry and radiative cooling for primordial gas are included with the code developed by Susa & Kitayama (2000), where  $\text{H}_2$  cooling and reaction rates are taken from Galli & Palla (1998). To solve radiative transfer in an SPH scheme, we employ the method proposed by Kessel-Deynet & Burkert (2000), which utilizes the neighbour lists of SPH particles to evaluate the optical depth from a certain source to an SPH particle.

To generate UV background radiation, we put a single ionizing source located very far from the simulated region, and control the UV intensity by specifying the incident flux to the simulation box. We assume the history of UV intensity that allows the early reionization inferred by *WMAP*. Since the recombination time scale is shorter than the Hubble expansion time at  $z \gtrsim 10$  (Peebles 1968), ionizing photons should be continuously supplied in order to retain the ionization. The requisite UV intensity is given by equating the recombination rate to ionization rate:

$$I_{\nu_L} = \frac{n_0(1+z)^3 k_{\text{rec}} h_P (\alpha + 3) (1 - y_{\text{HI}})^2}{4\pi\sigma_{\nu_L} y_{\text{HI}}}, \quad (1)$$

where  $I_{\nu_L}$  denotes the intensity at Lyman limit, and  $k_{\text{rec}}$ ,  $\sigma_{\nu_L}$ , and  $h_P$  respectively represent the recombination coefficient, ionization cross-section at Lyman limit, and Plank constant.  $n_0$  is the present-day baryon density,  $\alpha$  is the

spectral index of UV radiation, and  $y_{\text{HI}}$  is the fraction of neutral hydrogen. If  $y_{\text{HI}} = 0.1$  at  $z \simeq 15$ ,  $I_{21} \simeq 10^{-3}$  is required. This should be regarded as the minimal prerequisite for two reasons. First, this estimate is provided for optically-thin media. In actual ionization history, the radiative transfer effect is definitely important (Nakamoto, Umemura, & Susa 2001). Secondly, in an inhomogeneous universe, local density enhancements increase the recombination rate significantly. Taking these into account, we assume  $I_{21} = 0.01$  for  $5 < z < 17$  with a sharp decrease at  $z > 17$  as  $I_{21} \propto \exp[3(17 - z)]$ . Also, some models with  $I_{21} = 1$  are simulated to investigate the dependence on  $I_{21}$ .

The ‘‘star formation’’ condition adopted in this paper is basically the same as Susa & Umemura (2004), except that  $c_* = 1$  is assumed here.  $c_* = 1$  means the star formation at maximal feasible rate, because no stars can form in a timescale shorter than local free-fall time. Here, we do not include the internal feedback effects by stellar UV radiation as well as SN explosions.

We assume  $\Omega_M = 0.3$ ,  $\Omega_\Lambda = 0.7$ ,  $\Omega_{\text{baryon}} h^2 = 0.02$ , and  $h = 0.7$ , as the background cosmology. Following the density fluctuations in this cosmology, the initial distributions of particles are set up. The mass of virialized dark halo is in the range of  $10^6 M_\odot \lesssim M_{\text{vir}} \lesssim 10^8 M_\odot$ , and the collapse epoch is  $5 \lesssim z_c \lesssim 20$ . We use  $2^{15}$  SPH particles and  $2^{15}$  dark matter particles for a run.

## 3. RESULTS

The numerical results are summarized in Figure 1. The left panel shows the fraction of the final mass in stellar component to the initial baryon mass as a function of the collapse epoch  $z_c$  and  $M_{\text{vir}}$ , while the right panel is the final fraction of gas. In both panels, the fraction is depicted by different symbols. Dotted lines represent the collapse epoch of halos formed from  $1\sigma$ ,  $2\sigma$  and  $3\sigma$  CDM density fluctuations. Roughly 95% of fluctuations collapse after the epoch predicted by the  $2\sigma$  line. Dashed lines denote the constant circular velocities, which are defined by  $v_{\text{circ}} \equiv \sqrt{GM_{\text{vir}}/r_{\text{vir}}}$  with the virial radius  $r_{\text{vir}}$  determined by  $z_c$  and  $M_{\text{vir}}$ .

In Figure 1, we see that, if  $M_{\text{vir}} \gtrsim 10^8 M_\odot$  and  $v_{\text{circ}} \gtrsim 20\text{ km s}^{-1}$ , almost all baryons are transformed into stars, leaving little gas. It is noted that a considerable fraction of baryonic matter form stars even after the reionization ( $z_c < z_{\text{reion}} = 17$ ). On the other hand, if  $v_{\text{circ}} \lesssim 20\text{ km s}^{-1}$ ,  $f_{\text{star}}$  steeply decreases with decreasing circular velocities. Also,  $f_{\text{gas}}$  becomes quite small as seen in the right panel. This reflects the effect of photo-evaporation by the UVB. The dependence of photo-evaporation on  $M_{\text{vir}}$  and  $z_c$  is understood by the self-shielding and the gravitational potential. The self-shielding against UVB becomes prominent if the local density exceeds a threshold density as

$$n_{\text{shield}} = 1.4 \times 10^{-2} \text{ cm}^{-3} \left( \frac{M_{\text{baryon}}}{10^8 M_\odot} \right)^{-1/5} \left( \frac{I_{21}}{\alpha} \right)^{3/5} \quad (2)$$

(Tajiri & Umemura 1998). This means that the self-shielding is more effective if the system is larger or collapses at higher redshifts. The gas envelope that is not shielded from UVB is photo-heated to  $\lesssim 10^4\text{ K}$  and is blown out by the enhanced thermal pressure, unless the gravitational potential is deep enough to retain the ionized gas

(i.e.  $v_{\text{circ}} \gtrsim 20 \text{ km s}^{-1}$ ). Hence, the photo-evaporation is quite devastating for fluctuations with lower masses and later collapse epochs. Intriguingly, a steep transition of  $f_{\text{star}}$  for  $v_{\text{circ}} \lesssim 20 \text{ km s}^{-1}$  coincidentally lies on a line of nearly constant  $\sigma$ , i.e.,  $\delta\rho/\rho \approx 2\sigma$ . This means that in more than 95% of the halos with  $v_{\text{circ}} \lesssim 20 \text{ km s}^{-1}$ , the star formation is strongly suppressed by the early reionization.

In the present simulation, the star formation is assumed to proceed in local free-fall time. This leads to the physically maximal star formation rate. Hence, the obtained stellar fraction in a halo should be regarded as a maximal one. If the star formation proceeds in a longer timescale, baryon gas in a halo with  $v_{\text{circ}} \lesssim 20 \text{ km s}^{-1}$  could be almost completely photo-evaporated after the reionization. On the other hand, fluctuations with  $v_{\text{circ}} \gtrsim 20 \text{ km s}^{-1}$  is like to be impervious to the photo-evaporation, since the gravitational potential is deep enough to retain the ionized gas.

To examine the dependence of results on assumed UVB intensity ( $I_{21}$ ), we also perform several runs with  $I_{21} = 1$ . In this case, a steep transition of  $f_{\text{star}}$  is slightly shifted to higher  $\sigma$  as  $\delta\rho/\rho \approx 2.5\sigma$ . Thus, it turns out that the results are not strongly dependent on the UVB intensity. Such insensitiveness may be understood by the weak dependence of the self-shielding on the UV intensity seen in equation (2).

Finally, to check the numerical effects, we analyze the convergence of the runs with changing the mass resolution and softening length. In Figure 2, the left panel shows the final stellar fraction ( $f_{\text{star}}$ ) in runs with  $M_{\text{vir}} = 6 \times 10^7 M_{\odot}$  and  $z_c \simeq 10$ , while the right panel is with  $M_{\text{vir}} = 6 \times 10^6 M_{\odot}$  and  $z_c \simeq 15$ . They are at the transition region of  $f_{\text{star}}$  in Figure 1. The horizontal axis in Figure 2 is the softening length  $\epsilon$  for gravity. Four different curves correspond to the different numbers of particles used in the simulations. We can see that  $f_{\text{star}}$  almost converges, if  $N_{\text{SPH}} \gtrsim 2^{15}$  and if  $\epsilon \lesssim 10 - 20 \text{ pc}$ . Thus, the present simulation with  $\epsilon = 20 \text{ pc}$  and  $N_{\text{SPH}} = 2^{15}$  ( $= N_{\text{DM}}$ ) is unlikely to suffer from numerical effects.

#### 4. DISCUSSION

The present numerical simulations predict strong negative feedback on the formation of dwarf galaxies with  $v_{\text{circ}} \lesssim 20 \text{ km s}^{-1}$ . Based on  $f_{\text{star}}$ , we can make a rough

estimation of the mass-to-light ratios ( $M/L$ ) for finally formed galaxies. If we assume  $M_{\text{star}}/L = 3$  for stars in solar units,  $f_{\text{star}} = 0.01$  corresponds to  $M_{\text{vir}}/L = 2.6 \times 10^3$  and  $f_{\text{star}} = 0.1$  to  $M_{\text{vir}}/L = 2.6 \times 10^2$ . But, these values cannot be compared directly with the observed  $M/L$  of satellite galaxies, because a quite large fraction (typically more than 90 percent) of dark matter halos of satellites can be tidally stripped, as shown by Kravtsov, Gnedin & Klypin (2004). Thus, the eventual  $M/L$  of satellites is likely to decrease by a factor of 10, e.g.  $M/L = 2.6 \times 10^2$  for  $f_{\text{star}} = 0.01$ . Local Group dwarf galaxies (dSphs and dIrrs) exhibit a wide range of  $M/L$ , which is from a few up to  $\approx 100$  (van den Bergh 1999; Mateo 1998; Hirashita, Takeuchi, & Tamura 1998). Hence, the formed galaxies with  $f_{\text{star}} \gtrsim 0.01$  may account for the Local Group dwarf galaxies. The present simulation predicts that only a few percent of fluctuations result in  $f_{\text{star}} \gtrsim 0.01$ , if  $v_{\text{circ}} \lesssim 20 \text{ km s}^{-1}$ . If the star formation rate is lower, the probability is reduced further. Hence, such intrinsically low-mass halos may be too few to account for all Galactic satellites.

One possibility to reconcile this discrepancy could be a model suggested by Kravtsov, Gnedin & Klypin (2004). They found that 10% of small halos originate in considerably larger systems with  $\gtrsim 10^9 M_{\odot}$ , which survived the tidal stripping, and suggest that the Galactic satellites are descendants of relatively massive systems which formed at higher redshifts. In our simulation, systems larger than  $10^8 M_{\odot}$  are not subject to the UVB feedback. Thus, their model seems viable to account for the number of Local Group dwarf galaxies.

We are grateful to the referee, who provided helpful comments on this paper. We thank A. Ferrara, T. Kitayama, K. Omukai, K. Wada, N. Yoshida, and S. White for stimulating discussion. The HMCS has been developed in a project which Center for Computational Physics, University of Tsukuba propelled in the course of JSPS Research-for-the-Future program of Computational Science and Engineering. The analysis has been made with computational facilities at Center for Computational Sciences in University of Tsukuba and Rikkyo University. We acknowledge Research Grant from Japan Society for the Promotion of Science (15740122:HS, 15340060:MU).

#### REFERENCES

- Babul, A. & Rees, M. J. 1992, MNRAS, 255, 346  
 Barkana, R. & Loeb, A. 1999, ApJ, 523, 54  
 Benson, A., Frenk, C., Lacey, C., Baugh, C. & Cole, S. 2002 MNRAS, 333, 177  
 Boku, T., Makino, J., Susa, H., Umemura, M., Fukushige, T. & Ukawa, A. 2002, IPSJ Transactions on High Performance Computing Systems, 41, 5  
 Bond, J., Szalay, A. & Silk, J. 1988, ApJ, 324, 627  
 Bromm, V., Ferrara, A., Coppi, P. S. & Larson, R. B. 2001, MNRAS, 328, 969  
 Bullock, J., Kravtsov, A. & Weinberg, D. 2000, ApJ, 539, 517  
 Cen, R. 2003, ApJ, 591, 12  
 Dekel, A. & Silk, J. 1986 ApJ, 303, 39  
 Dijkstra, M., Haiman, Z., Rees, M., Weinberg, D. 2004 ApJ, 601, 666  
 Efstathiou, G. 1992 MNRAS, 256, 43  
 Efstathiou, G. 2000 MNRAS, 317, 697  
 Galli D. & Palla F. 1998, A&A, 335, 403  
 Hirashita, H., Takeuchi, T. T., & Tamura, N. 1998, ApJ, 504, L83  
 Kay, S., Pearce, F., Frenk, C. & Jenkins, A. 2002 MNRAS, 330, 113  
 Kessel-Deynet, O. & Burkert, A. 2000, MNRAS, 315, 713  
 Kitayama, T., & Ikeuchi, S. 2000, ApJ, 529, 615  
 Kitayama, T., Tajiri, Y., Umemura, M., Susa, H., & Ikeuchi, S. 2000, MNRAS, 315, 1  
 Kitayama, T., Susa, H., Umemura, M., & Ikeuchi, S. 2001, MNRAS, 326, 1353  
 Kogut, A. et al. 2003, ApJ, submitted (astro-ph/0302213)  
 Kravtsov, A., Gnedin, O. & Klypin, A., 2004, astro-ph(0401088)  
 Klypin, A., Kravtsov, A., Valenzuela, O., & Prada, F. 1999, ApJ, 522, 82  
 Makino, J. 2002, ASP Conf. Ser. 263: Stellar Collisions, Mergers and their Consequences, 389  
 Mateo, M. 1998, ARA&A, 36, 435  
 Marri, S. & White, S. 2002, MNRAS, 345, 561  
 Moore, B., Ghigna, S., Governato, F., Lake, G., Quinn, T., Stadel, J., & Tozzi, P. 1999, ApJ, 524, L19  
 Nakamoto, T., Umemura, M., & Susa, H. 2001, MNRAS, 321, 593  
 Peebles, P. J. E. 1968, ApJ, 153, 1  
 Ricotti, M., Gnedin, N. Y., & Shull, J. M. 2002, ApJ, 575, 49  
 Ricotti, M. & Ostriker, J. P. 2004, MNRAS, 350, 539  
 Somerville, R. 2002, ApJ, 572, 23  
 Steinmetz, M. & Müller, E. 1993, A&A, 268, 391

- Susa, H. & Kitayama, T. 2000, MNRAS, 317, 175  
Susa, H. & Umemura, M. 2004, ApJ, 600, 1  
Tajiri, Y. & Umemura, M. 1998, ApJ, 502, 59  
Thacker, J., Tittley, R., Pearce, R., Couchman, P. & Thomas, A. 2000, MNRAS319, 619  
Thoul, A. A. & Weinberg, D. H. 1996, ApJ, 465, 608  
Umemura, M. 1993, ApJ, 406, 361  
Umemura, M. & Ikeuchi, S. 1984, Progress of Theoretical Physics, 72, 47  
van den Bergh, S., 1999, A&ARv, 9, 273  
Wada, K. & Venkatesan, A. 2003, ApJ, 591, 38  
Yepes, G., Kates, R., Khokhlov, A. & Klypin, A. 1997, MNRAS, 284, 235

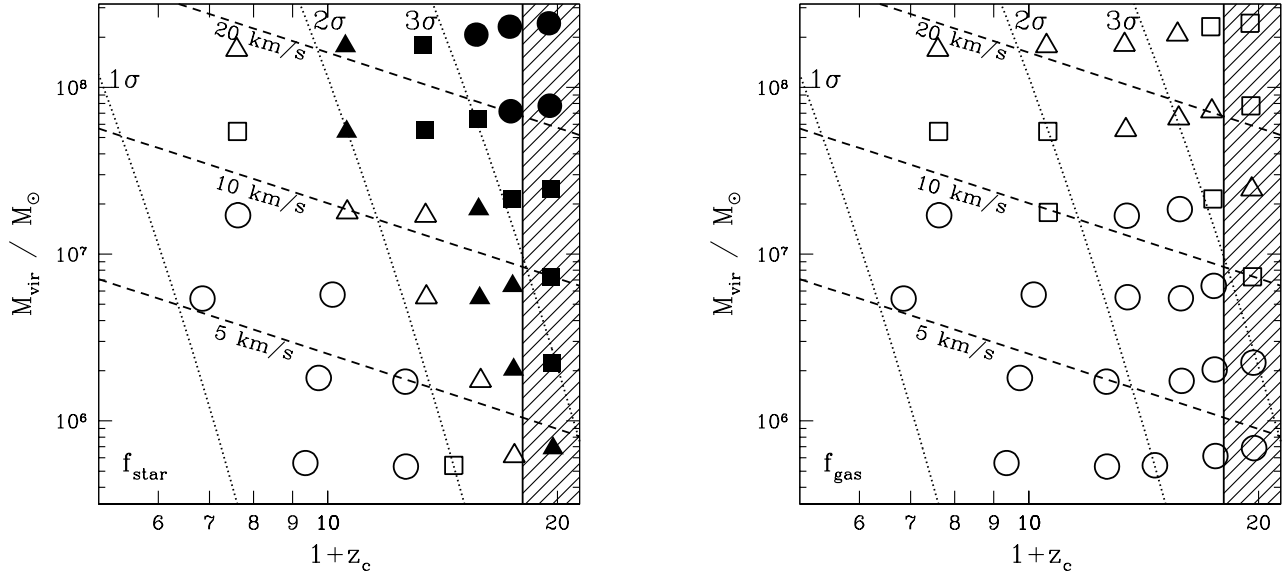


FIG. 1.— Summary of numerical runs are shown as a function of the collapse epoch  $z_c$  and the virialized halo mass  $M_{\text{vir}}$ . The left panel shows the fraction of the final mass in stellar component to the initial baryon mass, while the right panel is the final fraction of gas. In both panels, the fraction  $f$  is depicted by different symbols; *filled circles* are  $f > 0.9$ , *filled squares*  $0.5 < f < 0.9$ , *filled triangles*  $0.1 < f < 0.5$ , *open triangles*  $0.01 < f < 0.1$ , *open squares*  $10^{-3} < f < 0.01$ , and *open circles*  $f < 10^{-3}$ . Dotted lines represent the collapse epoch of halos formed from  $1\sigma$ ,  $2\sigma$  and  $3\sigma$  CDM density fluctuations. Dashed lines denote the constant circular velocities of 5 km/s, 10km/s, and 20km/s.

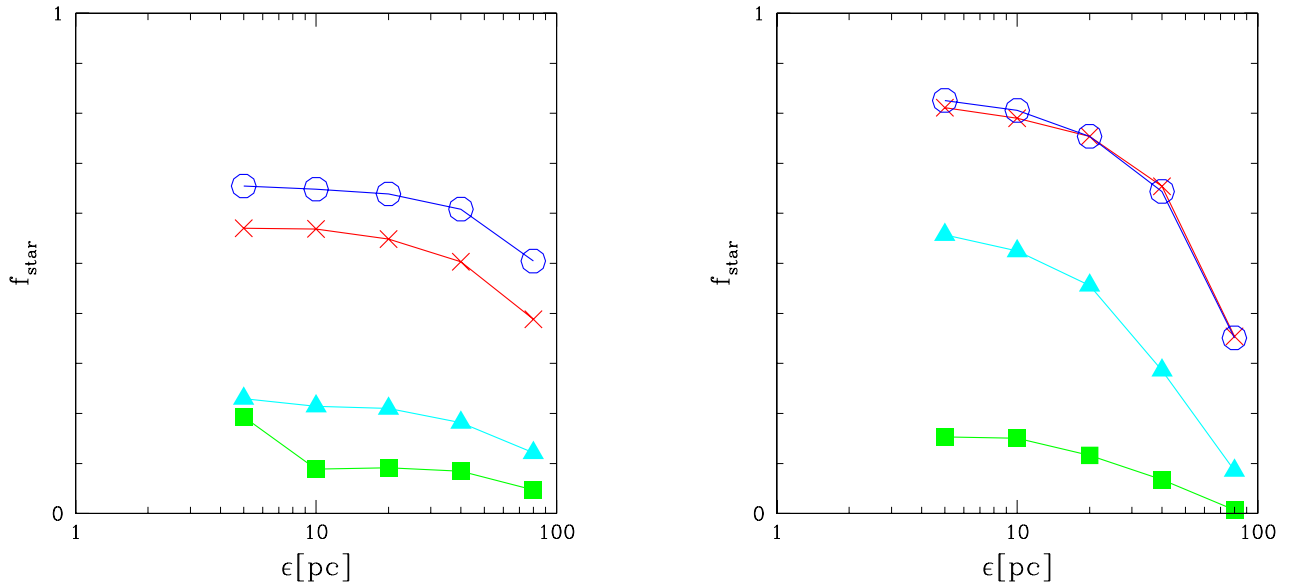


FIG. 2.— Convergence check of the numerical simulations. The left panel shows the convergence of runs with  $M_{\text{vir}} = 6 \times 10^7 M_{\odot}$  and  $z_c \simeq 10$ , and the right panel is for  $M_{\text{vir}} = 6 \times 10^6 M_{\odot}$  and  $z_c \simeq 15$ . In both panels, vertical axes represent the final stellar mass fraction, and the horizontal axes show the softening length of the gravitational force. Four different curves represent the results with various number of particles: *circles* denote  $N_{\text{SPH}} = 2^{17}$ , *crosses*  $N_{\text{SPH}} = 2^{15}$ , *triangles*  $N_{\text{SPH}} = 2^{14}$ , and *squares*  $N_{\text{SPH}} = 2^{13}$ .